Accepted Manuscript

1   # Ecotoxicological effects of transformed silver and

2   # titanium dioxide nanoparticles in the effluent from a

3   # lab-scale wastewater treatment system

4   *Anastasia Georgantzopoulou[†]*, Patricia Almeida Carvalho[‡], Christian Vogelsang[†], Mengstab*

5   *Tilahun[†], Kuria Ndungu[†], Andy M. Booth[□], Kevin V. Thomas[†,∥] and Ailbhe Macken[†]*

6   [†]NIVA, Norwegian Institute for Water Research, Gaustadalleen 21, 0349, Oslo, Norway

7   [‡]SINTEF Materials and Chemistry, Forskningsveien 1, 0373, Oslo, Norway

8   [□]SINTEF Ocean, Brattørkaia 17C, 7010, Trondheim, Norway

9   [∥]Queensland Alliance for Environmental Health Sciences (QAEHS), University of Queensland,

10   20 Cornwall Street, Woolloongabba, Queensland, 4102 Australia

11

12

13   ABSTRACT

14   In this study, a lab-scale wastewater treatment plant (WWTP), simulating biological treatment,

15   received 10 µg/L Ag and 100 µg/L TiO_2 nanoparticles (NPs) for five weeks. NP partitioning was

16   evaluated by size fractionation (>0.7 µm, 0.1-0.7 µm, 3 kDa-0.1 µm, <3 kDa) using inductively

17   coupled plasma mass spectrometry (ICP-MS), single particle ICP-MS and transmission electron

18   microscopy. The ecotoxicological effects of the transformed NPs in the effluent were assessed

19   using a battery of marine and freshwater bioassays (algae and crustaceans) and an *in vitro* gill

20   cell line model (RTgill-W1). TiO_2 aggregates were detected in the effluent, while Ag NPs (0.1 to

21   0.22 µg/L) were associated with S, Cu, Zn. Fractionation showed that >80% of Ag and Ti were

22   associated with the effluent solids. Increased toxicity was observed during weeks 2-3 and the

23   effects were species-dependent; with marine epibenthic copepods and algae being the most

24   sensitive. Increased reactive oxygen species formation was observed *in vitro* followed by an

25   increase in epithelial permeability. The effluent affected the gill epithelium integrity *in vitro* and

26   impacted defense pathways (upregulation of multixenobiotic resistance genes). To our

27   knowledge, this is the first study to combine a lab-scale activated sludge WWTP with extensive

28   characterization techniques and ecotoxicological assays to study the effects of transformed NPs

29   in the effluent.

30

31   INTRODUCTION

32   The production and use of consumer products containing Ag and TiO_2 NPs continues to

33   increase[1,2] and due to their widespread use and application they can enter sewage streams and

34   wastewater treatment plants (WWTPs). Their presence in the influent of WWTPs has been

35   reported in several studies[3–7]. Ag and TiO_2 NPs tend to be associated with particulate matter and

36   appear to be relatively efficiently removed from the wastewater during primary and secondary

37   treatment[3,4,6,8,9], the extent of removal however depends on the design and efficiency of the

38   operating conditions[6]. Ag-based and TiO_2 NPs have been detected in wastewater effluents[6,9]

39   making their release in surface waters through effluent discharge possible, which can potentially

40   be an important exposure route for aquatic organisms in receiving waters.

41   Nanoparticles undergo a combination of physical and chemical transformations in environmental

42   media (e.g. wastewaters)[10] that may influence their behavior, bioavailability and toxicity[11,12].

43   Their behavior may differ from their pristine NP counterparts, thereby making comparisons and

44   predictions between transformed and pristine NPs difficult. It has been reported that Ag NPs are

45   sulfidized to various degrees in wastewater streams and during transport to WWTPs[8,13].

46   Furthermore, studies using a pilot WWTP fed with municipal wastewater spiked with Ag NPs,

47   showed a transformation to Ag_2S while some of the Ag NPs detected in the effluent were still in

48   the pristine metallic form[14]. Even though most NPs present in the natural environment are likely

49   to have undergone some form of physicochemical transformation, very few effects studies have

50   employed transformed NPs[15–17] or NPs in environmentally relevant media such as

51   wastewaters[12,18,19]. One recent study has shown that Cu NP transformation through a septic tank

52   led to a lack of toxicity in a zebrafish embryo hatching assay[15]. A decreased toxicity was also

53   observed for the freshwater amphipod *H. Azteca* exposed to Ag NPs transformed through an

54   activated sludge simulation system[17] while another study showed an increased zebrafish embryo

55   toxicity in the effluent of a similar system dosed with 4-16 mg/L Ag NPs[20]. Studies using

56   sulfidized Ag NPs through wastewater treatment processes demonstrated that although Ag_2S NPs

57   are less soluble, they can still be bioavailable to different organisms[21,22] and induce toxicity,

58   though at lower levels compared to pristine Ag NPs[23]. This highlights the need of a better

59   understanding of the behavior of NPs, their transformation and their toxicity in complex media.

60   It remains a challenging task to detect and quantify NPs at low, but environmentally relevant

61   concentrations ($< \mu g/L$) in complex matrices such as wastewater, effluent, sewage sludge, and

62   surface waters[24]. As a result, most environmental fate studies and toxicological assessments are

63   conducted at much higher concentrations than those expected to be found in the environment[20],

64   and studies taking into account relevant exposures at more realistic conditions are scarce[15,16].

65   There is a need to develop a better understanding of the environmental impact of transformed

66   NPs at environmentally relevant concentrations[25].

67   The current study investigates the potential hazard of transformed Ag and TiO_2 NPs through

68   advanced biological treatment processes present in complex environmental media such as

69   WWTP effluents at environmentally relevant NP concentrations. A lab-scale pre-denitrifying

70   WWTP system with pre-conditioned activated sludge was established and continuously fed with

71   artificial wastewater dosed with 10 $\mu g/L$ Ag and 100 $\mu g/L$ TiO_2 NPs for a period of 5 weeks.

72   The system was combined with a battery of marine and freshwater bioassays and NP

73   characterization techniques to evaluate the hazard potential of transformed Ag and TiO_2 NPs.

74   Sequential filtration combined with ICP-MS was applied to characterize the different size

75   fractions (associated with settling solids, colloidal matter, nanoscale and dissolved). Both marine

76   (*Skeletonema pseudocostatum*, *Tisbe battagliai*) and freshwater (*Raphidocelis subcapitata*,

77   *Daphnia magna*) organisms (algae and crustaceans) were used as model species to monitor the

78   toxicity of the transformed NPs present in the effluent during the 5-week dosing period. The

79   choice of organisms reflects that the behavior of NPs differs in marine and freshwater

80   environments, the effects may vary depending on the species used[26] as well as the fact that in

81   many countries the effluent is discharged in both freshwater and marine environments.

82   Furthermore, an *in vitro* model using the rainbow trout (*Oncorhynchus mykiss*) gill cell line

83   RTgill-W1 was employed, representing a major interface between the organism and its

84   environment that is one of the first sites impacted by waterborne chemicals. The model was used

85   in addition to the standard bioassays for assessment of the effluent with minimal sample

86   modification during the period of dosing of the WWTP system and cellular responses were

87   assessed (metabolic activity, epithelial integrity, reactive oxygen species (ROS) formation and

88   the gene expression of zonula occludens-1 and multixenobiotic resistance genes ABCB1,

89   ABCC1 and ABCC2).

90

91   MATERIALS AND METHODS

92   **Nanoparticles and chemicals.** Polyvinylpyrrolidone (PVP)-coated Ag NPs (Econix 25 nm,

93   aqueous suspension) were obtained from Nanocomposix (Czech Republic). TiO_2 NPs (NM-101,

94   primary particles of 5 nm) were obtained from the Joint Research Centre (JRC Repository, Ispra,

95   Italy) and have been extensively characterized previously[27]. A stock dispersion of TiO_2 NPs in

96   0.22 μm filtered MilliQ (2.56 mg/ml) was prepared in a Scint-Burk glass vial and sonicated in

97   ice water for 13 min with a calibrated probe sonicator according to the FP7 EU NANoREG

98   sonication protocol[28]. The NP stock dispersions were then analyzed with scanning transmission

99   electron microscopy (STEM), single particle (sp-ICP-MS, see sections below) and dynamic light

100   scattering (DLS) (Supporting Information; SI). AgNO$_3$ (Sigma-Aldrich) was used as an ionic

101   control.

102   **Lab-scale wastewater treatment plant.** The lab-scale WWTP was a pre-denitrifying activated

103   sludge treatment system comprised of a 6.5 L non-aerated denitrifying reactor, an 8 L aerated

104   nitrifying reactor with automatic temperature (20°C) and pH (7.2) control and a 5.1 L settler (SI;

105   Figure S1). The activated sludge used in the system was collected from Bekkelaget WWTP,

106   Oslo, Norway. To adapt the activated sludge to the synthetic medium and to wash out any NPs

107   transferred to the system together with the initial sludge, the system was continuously fed

108   (hydraulic retention time ~15 h) synthetic wastewater without NPs for a period of 10 weeks. The

109   composition and characteristics of the synthetic wastewater and a detailed description of the

110   system operation and the parameters measured are presented in the SI. Sludge was continuously

111   removed from the denitrifying reactor to maintain a solids retention time (SRT) of ~15 days.

112   During the adaptation period effluent samples from the reference system without NPs were

113   collected weekly and served as "background controls". After the adaptation period the synthetic

114   medium was dosed with a continuous supply of 10 µg/L Ag NPs and 100 µg/L TiO$_2$ NPs to the

115   denitrifying reactor for a period of 5 weeks. The synthetic wastewater containing Ag and TiO$_2$

116   NPs was freshly prepared every 2-3 days. Effluent samples were collected weekly and used to

117   evaluate the influence of NP transformation on the battery of bioassays (performed within 48 h

118   of effluent collection). The COD and total inorganic N removal was 81±8 % and 71±16 %,

119   respectively (SI).

120   **Ag and TiO$_2$ NP characterization (STEM/EDS, sp-ICP-MS).** Ag, TiO$_2$ NP stock dispersions

121   or effluent samples were imaged using STEM, while elemental point analysis and mapping were

122 performed with energy-dispersive X-ray spectroscopy (EDS). A detailed description of the

123 STEM-EDS method is presented in the SI.

124 The effluent samples as prepared for STEM were transferred to Eppendorf tubes, vortexed for 30

125 s, sonicated for 30 min, and then diluted with MilliQ water prior to single particle ICP-MS (sp-

126 ICP-MS) analysis for particle concentration and size. The sp-ICP-MS analytical protocol and

127 data analysis (using the single particle RIKILT calculation tool[29], Wageningen, The Netherlands)

128 are similar to those described elsewhere[9,29] (detailed description of the sp-ICP-MS method in SI).

129 **Ag and TiO$_2$ fractionation (filtration, ultrafiltration and ICP-MS).** Samples from the

130 influent, nitrifying and denitrifying reactors, as well as the effluent (collected from the overflow

131 of the settler), were collected weekly and fractionated using a series of membranes with

132 decreasing pore size immediately upon sample collection. The samples were filtered sequentially

133 through a 0.7 μm filter membrane (glass microfiber GF/F, Whatman, GE Healthcare Life

134 Sciences), a 0.1 μm membrane (Durapore membrane filter, Millipore) and finally centrifuged

135 through a 3 kDa cut-off membrane (Amicon Ultra-15, Millipore, 5000g for 1 h) to obtain the

136 soluble fraction present in the filtrate sample. The 0.7 μm filters were dried at 45°C for 2 h and

137 kept in microwave tubes until further analysis (solid-associated fraction or particles >0.7 μm).

138 The solids-associated (>0.7 μm), particulate (0.1-0.7 μm), NP (3 kDa cut-off - 0.1 μm) and the

139 soluble fraction (3 kDa filtrate) were analyzed by ICP-MS (see SI for details).

140 *Skeletonema pseudocostatum* **growth inhibition assay.** The marine algae were cultured in ISO

141 media[30] prepared from filtered natural seawater (35 ppt salinity), and maintained at 20°C under

142 continuous light and shaking according to the ISO 10253 standard. Dilution water used for the

143 exposure assays was a modified version of the ISO media with a reduced concentration (1/5) of

144   trace elements and EDTA to minimize free metal ion complexation[31] and possible impacts on the

145   toxicity profile of the effluent. The effluent was spiked with concentrated ISO media stock

146   solutions to reach the elemental concentrations present in the dilution water. Artificial sea salts

147   (Coral Pro Salt) were added to reach 35 ppt salinity. Increasing concentrations (5 concentrations:

148   6.2-100%) of effluent or pristine NPs and $AgNO_3$ were placed in a 12-well plate (1.35 ml/well,

149   triplicates). Exponentially growing algae were counted with a hemocytometer and 150 µl of

150    $1 \cdot 10^5$ cells/ ml were added to each well (final algal concentration $1 \cdot 10^4$ cells/ml). An artificial

151   seawater control was prepared by spiking artificial sea salts (to achieve 35ppt) into clean dilution

152   water. Filtered natural seawater with reduced trace elements and EDTA concentrations served as

153   an untreated control while "background" effluent control was also included. The algal cell

154   density and growth was assessed daily for 72 h by measuring fluorescence (excitation 530 nm:

155   emission 685 nm, Victor[3] Multilabel plate reader, PerkinElmer). The specific growth rate

156   (logarithmic increase in biomass) and the percent growth inhibition over the exposure period was

157   calculated according to the ISO standard.

158   ***Raphidocelis subcapitata* growth inhibition assay.** The freshwater algae were cultured in EPA

159   media[32] and maintained at 20°C under continuous light and shaking according to the OECD 201

160   guideline. The effluent was spiked with concentrated nutrient stock solutions to achieve the same

161   concentration as the standard media. Trace elements and EDTA were used at a reduced

162   concentration (1/5). 1.35 ml of increasing concentrations of effluent (5 concentrations: 6.2-

163   100%), pristine NPs or $AgNO_3$ were placed in a 12-well plate. Finally, 150 µl of algae ($5 \cdot 10^5$

164   cells/ml) in exponential growing phase were added per well (final algae concentration $5 \cdot 10^4$

165   cells/ml). Dilution water (MilliQ water supplemented with the concentrated stock solutions and

166   1/5 trace elements-EDTA) served as an untreated control and effluent collected during the

167 stabilization period served as a "background" effluent control. The algal cell number and growth

168 was measured daily for 72 h (fluorescence measurement, excitation 485 nm: emission 685 nm,

169 Victor[3] Multilabel plate reader, PerkinElmer).

170 **Effects of effluent on ROS formation (marine and freshwater algae).** Exponentially growing

171 algae were centrifuged and re-suspended in dilution water to achieve a concentration of $4 \cdot 10^6$

172 cells/ml. 25 µl of cell suspension was placed in each well of a 96-well plate (final algal

173 concentration $1 \cdot 10^6$ cells/ml) and incubated in the dark with 25 µl DCFH-DA 20 µM (final

174 concentration 10 µM) for 1.5 h under shaking conditions. At the end of the incubation period,

175 150 µl of effluent (serially diluted in dilution water) was added to each well and incubated for 1

176 h. At the end of the exposure period, DCF fluorescence was measured at wavelengths of 485 nm

177 excitation and 535 nm emission. H_2O_2 was used as a positive control.

178 ***Daphnia magna* acute toxicity assay.** Daphnids were maintained in M7 media[33] and fed with *R.*

179 *subcapitata* every other day. Daphnids <24 h old were used for the assay, which was performed

180 in 6-well plates as previously described[34] and according to OECD 202 guideline. Five daphnids

181 per well were used in quadruplicate and were exposed to increasing concentrations of effluent (5

182 concentrations: 6.25-100%). Moderately hard EPA water was used for dilutions of the effluent[35].

183 Daphnids in EPA water served as an untreated control while exposure to effluent collected

184 during the stabilization period served as a "background" effluent control. The effects of pristine

185 Ag NPs as well as spiked in background effluent (0.005-0.32 mg/L) were also evaluated.

186 Daphnid mobility was assessed after 24 and 48 h.

187 ***Tisbe battagliai* acute toxicity assay.** *T. battagliai* were maintained in filtered (0.22 µm)

188 seawater obtained from the outer Oslofjord and fed a mixed diet of *Rhodomonas baltica* and

189   *Isochrysis galbana.* Copepods of 6 ± 2 days old were used for the assay as previously

190   described[36]. Tests were performed in 12-well plates with 5 animals (4 replicates per treatment) in

191   each well containing ~4 ml of test solution. Artificial salts (Coral Pro Salt) were added to the

192   effluent to reach a salinity of 35 ppt, with further dilutions made in the natural seawater used for

193   culture maintenance. The effects of increasing concentrations of the effluent (5 concentrations:

194   6.25-100%), Ag NPs (0.08-1.3 mg/L), TiO_2 NPs (0.01-10 mg/L) or $AgNO_3$ (0.01-0.16 mg/L) in

195   seawater or spiked in background effluent were assessed after 24 and 48 h of exposure. MilliQ

196   water spiked with artificial sea salts acted as an artificial seawater control. Natural seawater

197   served as an untreated control.

198   **RTgill-W1 *in vitro* model in transwell inserts.** The rainbow trout gill epithelial cell line RTgill-

199   W1[37] was provided by Prof. Kristin Schirmer (EAWAG, Switzerland). Cells were cultured in

200   Leibovitz's L-15 medium (L-15, Gibco, ThermoFischer Scientific) supplemented with 5% fetal

201   bovine serum (FBS, Gibco, ThermoFischer Scientific) and 1% gentamicin solution (10 mg/ml,

202   Sigma-Aldrich), and maintained at 19 °C in an incubator in the absence of CO_2. The cells were

203   seeded in 12-well transwell inserts (Millicell Hanging Cell Culture Insert, 1.0 µm, Merck

204   Millipore) at a concentration of $1.8 \cdot 10^5$ cells/ml (0.5 ml cell suspension/insert). The basolateral

205   compartment was filled with 1.5 ml of complete L-15 cell culture medium in a 12-well receiver

206   plate (Merck Millipore). Cells were allowed to grow for 10 days and form a confluent

207   monolayer. The media was renewed every other day.

208   **Metabolic activity and epithelial integrity.** On day 10, the cells were exposed for 24 h to

209   increasing concentrations of the freshly collected effluent from the system (filtered through a 0.2

210   µm filter; serial dilutions with a dilution factor of 2), the pristine NPs or $AgNO_3$. Dilutions were

211   performed in L15/ex media as previously described[37,38]. Cells in L15/ex media served as an

212   untreated control. At the end of the exposure period the media was removed and replaced with

213   L15/ex media containing 100 μM alamar blue solution. Cells were incubated for 1 h and

214   fluorescence was measured at wavelengths of 530 nm excitation and 590 nm emission (Victor[3]

215   Multilabel plate reader, PerkinElmer). The alamar blue solution was then removed and replaced

216   with 0.1 mg/ml lucifer yellow (LY, Sigma-Aldrich) solution as a marker for paracellular

217   permeability. The cells were incubated for 2 h before the inserts were removed from the receiver

218   plates and fluorescence was measured at wavelengths of 485 nm excitation and 535 nm emission

219   (Victor[3] Multilabel plate reader, PerkinElmer).

220   **Quantitative real time PCR (qPCR).** After exposure of the RTgill-W1 cells in transwell

221   inserts, the exposure medium was removed, the cells were washed in PBS and were collected

222   with 300 μl RLT plus buffer (Qiagen) supplemented with 1% mercaptoethanol. Total RNA was

223   extracted using RNeasy Plus Mini Kit (Qiagen) according to the manufacturer´s instructions and

224   as previously described[39]. The RNA purity and concentration were determined using a Nanodrop

225   ND1000 spectrophotometer while RNA integrity was determined with an Agilent Bioanalyzer

226   RNA 6000 nano series kit (Agilent technologies, USA). The qPCR was performed as previously

227   described[39] (protocol details can be found in SI).

228   **Effects of effluent on ROS formation (*in vitro*).** RTgill-W1 cells were seeded in 96-well plates

229   at a concentration of $5 \cdot 10^5$ cells/ml (100 μl cell suspension/well). After 24 h, the media was

230   removed and fresh media containing 25 μM DCFH-DA in L15/ex media was placed in each well

231   (100 μl solution/well). After a 1 h incubation, the DCFH-DA solution was removed and replaced

232   with increasing concentrations of effluent (5 concentrations: 6-100%), Ag NPs, TiO_2 NPs or

233    $AgNO_3$ diluted in L15/ex. Fluorescence was measured after 1 and 2 h of exposure at wavelengths

234   of 485 nm excitation and 535 nm emission. H_2O_2 was used as a positive control.

235 **Statistical analysis.** Statistical analysis was performed with GraphPad Prism 6 (GraphPad

236 Software, La Jolla, CA 92037, USA). Values are expressed as means ± standard deviation.

237 Significant differences between the different treatments and control were analyzed with one-way

238 analysis of variance (ANOVA) followed by Dunnet´s multiple comparison test or nonparametric

239 Kruskal-Wallis test followed by Dunn's multiple comparison test. Statistical significance was

240 defined at $p < 0.05$. Dose-response curves, EC_{10} and EC_{50} values were obtained with GraphPad

241 Prism 6 (GraphPad Software, La Jolla, CA 92037, USA) using a logistic four-parameter model.

242 Principal component analysis (PCA) of the parameters and effects observed with the different

243 bioassays was performed with XLSTAT 2018 (SI).

244 **RESULTS AND DISCUSSION**

245 **Ag and TiO$_2$ Nanoparticle characterization.** The physicochemical properties determined for

246 the Ag and TiO$_2$ NP stock dispersions in MilliQ water are summarized in the SI (Figures S2-3,

247 Table S1). The Ag NPs were spherical with a mean diameter of 26.5 ± 0.7 nm and 58.8 ± 0.19

248 nm according to sp-ICP-MS and DLS measurements, respectively. DLS and sp-ICP-MS analyses

249 showed an average TiO$_2$ aggregate size of 640.7 ± 9.2 and 278 ± 15 nm, respectively. STEM

250 imaging indicated that TiO$_2$ NPs were porous and formed large aggregates consisting of

251 individual particles below 10 nm, confirming previous reports on this material[27]. In synthetic

252 wastewater and seawater TiO$_2$ aggregates of 969 ± 19 nm and 1375 ± 76.7 nm, respectively were

253 measured with DLS (SI; Table S1). Ag NPs in synthetic wastewater, seawater and the exposure

254 media used in the bioassays ranged from 57.3 ± 0.17 to 59.5 ± 0.18 nm as measured with DLS,

255 suggesting a stability of the PVP-coated Ag NPs in the different media. The higher (~2x) particle

256 size obtained for both pristine Ag NPs and TiO$_2$ with DLS is probably related to the inherent

257 properties of the instrument, light scattering techniques such as DLS require higher

258   concentrations that can result in aggregation that could influence the analytical signal[40]. With sp-

259   ICP-MS low concentration levels can be detected in more complex or natural environmental

260   samples. Therefore, multiple analytical techniques are necessary especially for low NP

261   concentrations in environmental samples.

262   **Ag and TiO$_2$ NP transformation in the lab-scale WWTP.** Sequential filtration and ICP-MS

263   analysis of the individual effluent fractions showed that >80% of the Ag and Ti measured was

264   associated with suspended solids (>0.7 μm fraction) present in the effluent samples (Figure 1,

265   Figure S4). The highest concentrations of both total Ag and Ti were observed in effluents from

266   weeks 2 and 5. The Ti levels in the fraction >0.7 μm ranged from 0.9-24.2 μg/L, with the highest

267   concentration measured at week 2. The dissolved Ag concentration was in the range of 0.005-

268   0.021 μg/L (Table 1). The highest dissolved Ag concentrations were observed in effluents

269   collected after 1 and 3 weeks of NP dosing, and corresponded to 7-8% of the total Ag measured

270   during those weeks. The Ag concentration present in the NP fraction ranged from 0.1-0.22 μg/L,

271   with the highest concentrations measured in the effluent samples collected in weeks 1, 3 and 5

272   (0.22, 0.14 and 0.17 μg/L, respectively). The Ti present in the 0.1 μm and 3 KDa fractions could

273   not be distinguished and quantified separately, therefore the values are reported as Ti >0.7 μm

274   and <0.7 μm. A previous study with sequencing batch reactors showed that a significant fraction

275   of Ag was associated with colloidal material (below 0.45 μm)[41] and biosolids in the sludge and

276   effluent of a pilot WWTP[14].

277

278
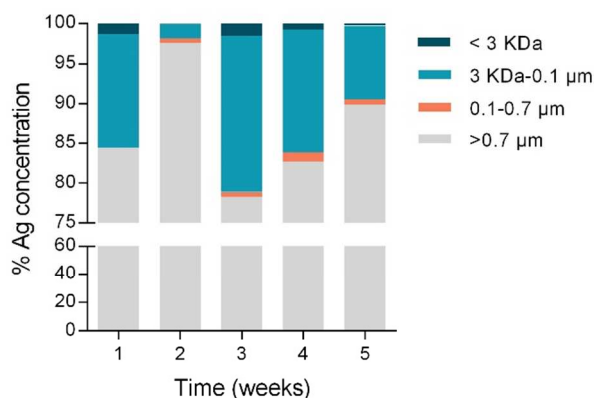
Figure 1. Effluent characterization and distribution of the total Ag present in the effluent of the lab-scale WWTP system during the 5 weeks of continuous dosing of the system.

281

Table 1. Ag and Ti concentrations (µg/L or µg/g effluent suspended solids) in each effluent fraction during the 5 weeks of operation and continuous dosing of the lab-scale WWTP system.

| | Ag concentration | | | | | | | | Ti concentration | | | |
| | Total | | >0.7 µm | | nano-Ag | | 3 KDa filtrate | | >0.7 µm | | <0.7µm | |
Effluent Sample	µg/L	µgAg/gSS	µg/L	µgAg/gSS	µg/L	µgAg/gSS	µg/L	µgAg/gSS	µg/L	µgTi/gSS	µg/L	µgTi/gSS
wk 1	0.74	47.34	0.51	32.21	0.22	13.82	0.02	1.31	0.90	57.50	0.14	8.67
wk 2	5.99	72.15	5.84	70.41	0.11	1.28	<0.005	0.06	24.20	291.52	0.13	1.55
wk 3	0.72	66.28	0.56	51.88	0.14	12.98	0.01	1.01	1.00	92.17	0.16	14.81
wk 4	0.65	47.90	0.54	39.60	0.10	7.37	<0.005	0.37	2.50	183.15	0.10	7.50
wk 5	1.80	333.22	1.62	299.75	0.17	30.59	<0.005	0.93	5.40	999.30	0.15	27.04

284

The effluent collected during the 4th week of system operation was analyzed by STEM in combination with EDS to determine both the presence and transformation of Ag and TiO_2 NPs. Electron microscopy images showed the presence of particles with high mass (bright contrast), while EDS analysis indicated that Ag-rich particles were associated with S, Cu and Zn (Figure 2A). STEM also showed the presence of TiO_2 polycrystalline aggregates (~50 nm) (Figure 2B)

290   comprised of primary particles below 10 nm which were similar to the initially dosed particles.

291   The association of Ag present in WWTP with elements such as Cu, Zn and S is in accordance

292   with previous studies reporting the presence of Ag particles associated with S in sludge[14,42] and

293   effluent samples[14]. It has recently been shown that secondary nano-sized Ag particles of

294   approximately 20 nm diameter associated with S from organic or inorganic source are formed

295   from dissolved silver from Ag NPs (80 nm, PVP coated) in batch systems with wastewater

296   effluent and mixed liquor[10].
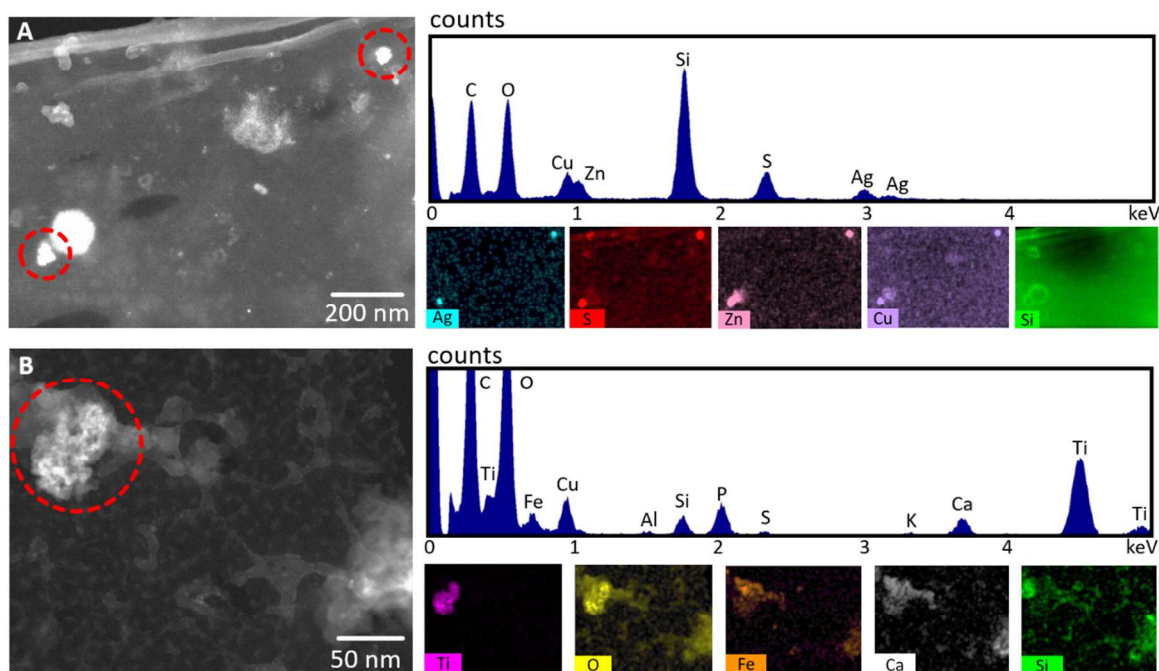
297

298   **Figure 2.** STEM images of (A) Ag-rich and (B) TiO_2 particles from the lab-scale WWTP,

299   together with sum spectra of the encircled regions and elemental maps. Particles were detected in

300   the effluent collected during the 4th week of dosing and operation of the system.

301

302   Single particle ICP-MS analysis of effluent samples collected during the 5 weeks of operation of

303   the system confirmed the presence of Ag and TiO_2 NPs, indicating they occurred within the size

304   ranges 20.5-31.6 nm and 110.9-124.8 nm, respectively (SI; Table S1). Sp-ICP-MS is a very

305   promising technique for the identification and quantification of metallic NPs in complex

306   matrices[43], including wastewater and effluents[44–46]. The technique has low detection limits[47] and

307   requires highly diluted samples that are very relevant for environmental samples, as well as when

308   realistic exposures are to be studied. However, distinction between Ag complexes and species or

309   Ag bound colloids cannot be made[45].

310   **Effects of effluents on algal growth and ROS formation.** A 20-40% growth inhibition of the

311   marine algae, *S. pseudocostatum,* was observed upon exposure to effluents at the highest effluent

312   concentration (100%; Ag and Ti exposure concentrations of 6 and 24 µg/L, respectively), with

313   effluent from week 2 showing the strongest effect (40% growth inhibition relative to untreated

314   control) (Figure 3). However, results from the DCFH-DA assay indicated that no formation of

315   ROS occured for any of the tested effluents (SI; Figure S5). Exposure to the background effluent

316   alone did not result in any significant effect on algal growth. These concentrations are below the

317   respective no effect concentration (NOEC) values obtained for *S. pseudocostatum* in this study (1

318   mg/L and 10 mg/L for Ag and TiO_2 NPs). This suggests that the presence of solids and elevated

319   NH_4 concentrations (3.3 mg/L) contribute to the observed effects and not just the total Ag and Ti

320   present in the effluents (Table S2, Figure S8). Differences in toxicity of Ag NPs aged in crude

321   and final wastewater have been reported and decreased toxicity was related to the sample

322   physicochemical parameters and increased complexity[48].

323
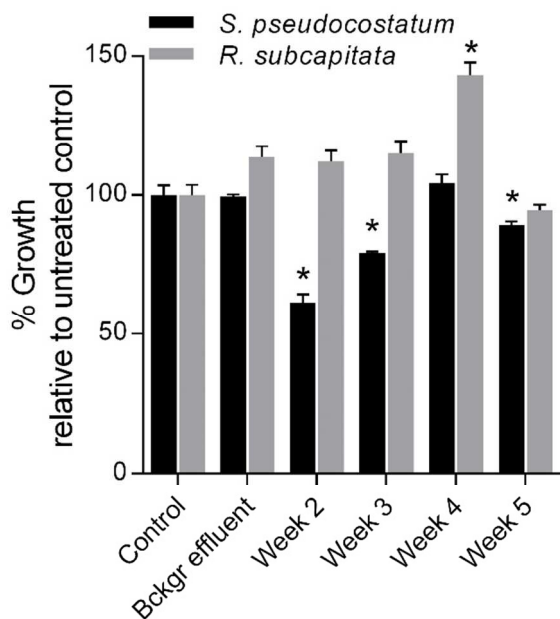
Figure 3. Percentage growth of *S. pseudocostatum* (black bars) and *R. subcapitata* (grey bars)

exposed to effluents collected in weeks 2-5 (100% and 50% effluent concentration for *S.*

pseudocostatum and *R. subcapitata*, respectively) and the background effluent. Algal growth

inhibition was determined after 72 h of exposure. Asterisks denote statistical significance at

$p < 0.05$.

In contrast to the inhibitory effects of the effluent on *S. pseudocostatum* growth, there was

evidence of hormetic effects in the freshwater algae, *R. subcapitata* exposed to effluent

concentrations <50%. These effects were most apparent after exposure to effluent collected from

week 4 and showed significant stimulatory effects on growth compared to the control (40%

increase in growth compared to control) (Figure 3). The stimulatory effects in *R. subcapitata*

growth were accompanied by a significant increase in the ROS formation (1.6-1.9-fold compared

to untreated control) (SI; Figure S5) and increased cell aggregation (observed by microscopy,

337   data not shown). The ROS formation was positively correlated with the total Ag and Ti

338   concentration, total N and suspended solids present in the effluents (Figure S8). A similar

339   response of cell aggregation has been previously reported upon exposure of the green algae

340   *Chlamydomonas reinhardtii* to CuO-polystyrene core-shell NPs[49] and *Chlorella vulgaris* and

341   *Dunaliella tertiolecta* to Ag NPs[50]. It has been suggested that cell aggregation is a defense

342   mechanism that decreases the amount of exposed surface to xenobiotics. Moderate stress and low

343   ROS levels can lead to hormetic effects that can in turn induce the defense system[51]. The results

344   from the current study indicate that responses to the effluent exposure are species-dependent,

345   possibly due to differences in cell size, surface area and cell wall composition. Studies with

346   green algae and cyanobacteria exposed to Ag NPs have also shown differences in cell viability

347   and ROS response between species attributed to different biological properties and the

348   production of extracellular polymeric substances[52]. Moreover, the NP behavior depends on the

349   media composition that can result in different responses, TiO_2 aggregates of 1369 nm were

350   observed in the presence of Cl in the higher ionic strength media of *S. pseudocostatum* compared

351   to 650 nm aggregates in *R. subcapitata* media while the Ag NPs seemed to be stable in both

352   media. The formation of insoluble AgCl(s) and dissolved silver chloride species depends on the

353   Cl/Ag ratio[53] which could further explain differences in effects observed between the freshwater

354   and marine algae.

355   **Effects of effluents on *T. battagliai* and *D. magna*.** Exposure to effluents collected weekly

356   during the operation of the system led to a 20-45% increase in mortality of *T. battagliai* (at 100%

357   effluent concentration), while no effect was observed from the background effluent (Figure 4A).

358   The highest significant mortality was observed upon exposure to effluents collected in weeks 2

359   and 5 (35 and 45% mortality compared to untreated control, respectively). Spiking the

360   background effluent with increasing concentrations of Ag NPs elicited a reduction in toxicity at

361   the lowest Ag NP concentration (0.08 mg/L) compared to pristine Ag NPs, but still caused a

362   significant increase in mortality at most concentrations (Figure 4B). Spiking the background

363   effluent also resulted in a 1.9x increase in the EC_{50} value compared to the pristine Ag NPs (0.09

364   and 0.17 mg/L, respectively) although the EC50 values were not statistically significant (Figure

365   4B). TiO_2 NPs did not have any effect on mortality at any of the concentrations tested (0.01-10

366   mg/L).

367   Although the total Ag concentration in the effluents (5.99 µg/L or 72.15 µg/gSS) exceeded the

368   NOEC for Ag NPs (0.005 mg/L), and was at a similar level to the EC_{10} obtained in this study

369   (0.0076 mg/L), no adverse effects on daphnid mobility were observed following 48 h exposure to

370   either the effluents or the background effluent. Spiking of the background effluent with

371   increasing concentrations of Ag NPs led to a significant decrease in mobility, but resulted in an

372   16x increase in the EC_{50} value compared to the pristine Ag NPs (0.16 and 0.0098 mg/L,

373   respectively) (Figure 5). TiO_2 NPs did not affect daphnid mobility.
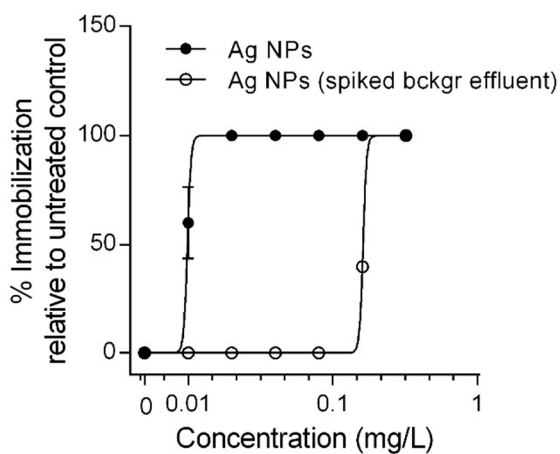
374
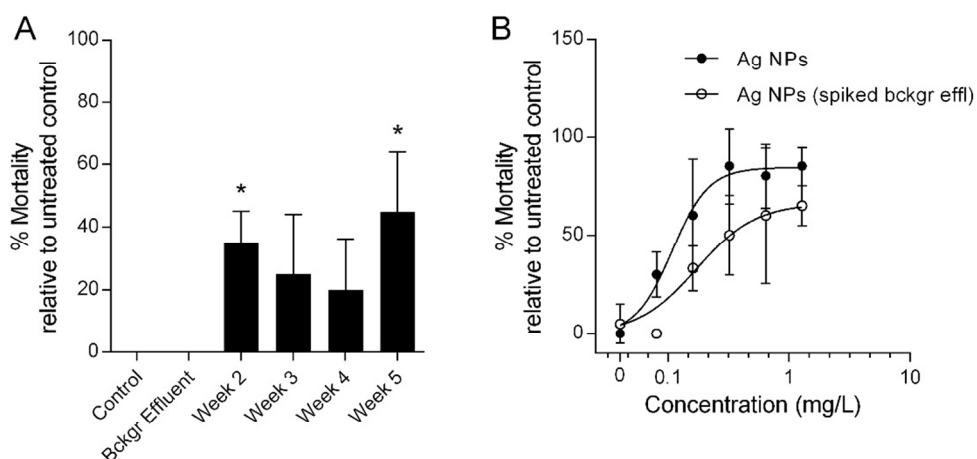
375

376 **Figure 4**. Percentage mortality of *T. battagliai* following 48 h exposure to (A) effluents collected

377 in weeks 2-5 and (B) increasing Ag NP concentrations as received or spiked in the background

378 effluent. Asterisks denote statistical significance at $p < 0.05$.

379

380

381 **Figure 5.** Percentage immobilization of *D. magna* juveniles following 48 h exposure to

382 increasing Ag NP concentrations and Ag NP-spiked background effluent. Background effluent

383 was collected during the system stabilization period (prior to spiking). No effects of effluents

384 collected in weeks 2-5 and background effluent were observed.

385

386   A clear reduction in the toxicity of Ag NPs to *D. magna* was observed when exposed to the

387   effluent collected from the lab-scale WWTP system (containing transformed Ag NPs) compared

388   to pristine Ag NPs. Unlike *D. magna*, the marine copepod *T. battagliai* exhibited a clear

389   response following exposure to the week 2-5 effluents (statistically significant in weeks 2 and 5).

390   The difference in response between the two species may result from a combination of NP

391   behavior in more complex WWTP effluents and differences in the feeding behavior of the two

392   organisms. *D. magna* is a planktonic filter feeding organism[54] while *T. battagliai* is an

393   opportunistic feeding epibenthic organism[55]. Therefore, *T. battagliai* is likely to be directly in

394   contact with particles associated with effluent solids that may settle out during the exposure

395   period. *T. battalgiai* are non-selective grazers as well as filter feeders and feed on suspended

396   particles along with detritus that settles out of the water column[56]. These differences in feeding

397   habit could explain the increased sensitivity of the copepods compared to daphnids when

398   exposed to the WWTP effluent. In contrast to this *D. magna* was 10x more sensitive to pristine

399   Ag NPs compared to *T. battagliai* (Figure 4 and 5). Therefore, the complete absence of effects in

400   *D. magna* exposed to any of the collected effluents reinforces the idea that NPs present in the

401   effluent are associated with the solids settling on the bottom of the vessels, reducing direct

402   exposure and ingestion by the daphnids.

403   To further confirm this, *T. battagliai* and *D. magna* were exposed to the background effluent

404   spiked with increasing concentrations of Ag NPs which led to decreased toxicity relative to the

405   pristine Ag NPs. However, for *T. battagliai* the EC_{50} value only increased 2 times, whereas for

406   *D. magna* the EC_{50} value increased 16 times. This indicates the presence of solids in the effluent,

407   as well as the potential formation of precipitates, reduces the bioavailability of the Ag NPs to the

408   daphnids compared to *T. battagliai*. This is in accordance with previous studies where reduced

409   toxicity of $AgNO_3$ spiked into untreated effluent was observed for the freshwater green algae *C.*

410   *reinhardtii*[19] and the protective effects of background effluent were observed towards Cu

411   interference with zebrafish hatching[15]. Furthermore, a decrease in the bioavailability of Ag from

412    $AgNO_3$-exposed algae (*C. reinhardtii*) was observed in wastewaters, and suggested to be due to

413   the presence of ligands[12]. It has been previously demonstrated that sulfidation[53], the presence of

414   natural organic matter[57] and thiol- or selenide-containing compounds such as cysteine[58] can

415   reduce the Ag NP dissolution rate and lead to protective effects due to Ag^+ complexation and

416   decreased bioavailability[59,60], partially explaining the reduced toxicity of Ag NPs spiked in

417   background effluent. The differences in EC50 increase trends of Ag NP-spiked background

418   effluent compared to pristine Ag NPs between the 2 organisms can also be attributed to

419   differences in media composition and ionic strength. The formation of AgCl precipitates in

420   media with high Cl content such as in seawater can further impact the Ag^+ availability and

421   subsequent toxicity[53,61]. Species-specific differences were related to the degree of Ag NP

422   sulfidation, the exposure route and species sensitivity[53].

423   Therefore, the effects of Ag NPs observed in the current study are considered organism-

424   dependent, with (epi)benthic organisms having the highest exposure risk due to directly ingesting

425   sedimented and aggregated NPs or NPs bound to effluent solids. In addition, the media

426   composition can impact the NP speciation and behavior leading to increased TiO_2 NP

427   aggregation and formation of silver chloride species in media of increasing ionic strength.

428   **Effects of effluents on RTgill-W1 cells.** The *in vitro* fish gill cell line model was employed in

429   the current study as the gill is a key site for xenobiotic uptake and it is continuously exposed to

430   water-borne contaminants[62]. Furthermore, the gills express enzymes involved in xenobiotic

431   metabolism and transport. Exposure to the 1-5 week effluents did not cause a statistically

432   significant decrease in the metabolic activity of RTgill-W1 cells in transwell inserts (Figure 6). A

433   40% decrease in the epithelial integrity (Figure 6), which coincided with a 2-fold increase in

434   ROS formation (Figure S6), was observed upon exposure to effluent from week 3. However, no

435   statistically significant effect was observed for any of the other effluents and no effect was

436   observed for the "background" effluent for either endpoint. Previous studies have shown that

437   primary fish gill cell cultures in permeable filter supports can tolerate apical water and varying

438   osmotic conditions[63], river water[64], detect bioreactive metals[64,65], and have been used to study the

439   uptake and transport of Ag NPs[66]. In the current study, it has proven to be a good model system

440   for whole effluent toxicity testing without the need for sample modification or alteration of the

441   water chemistry prior to exposure. However, the concentrations of Ag and TiO_2 NPs measured in

442   the effluent are considered too low to fully account for the effects observed in the metabolic

443   activity and epithelial integrity assays. Given the complexity of the wastewater effluent, it

444   appears that the combination of the presence of Ag NPs, ionic Ag and additional stressors such

445   as NO_3 contribute to the overall response observed (Figure S8).

446

447
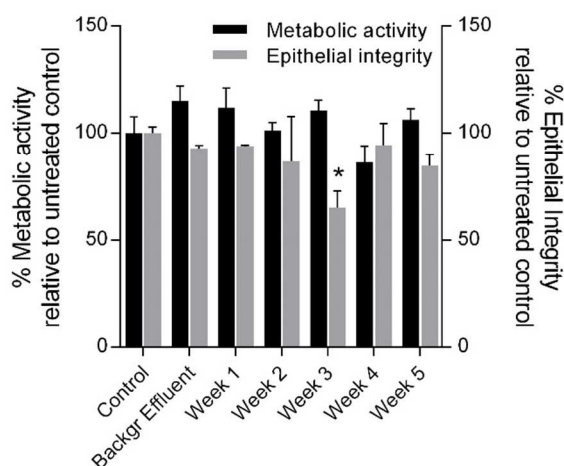
448

449   **Figure 6.** Percentage change in metabolic activity (left Y axis, black bars) and epithelial integrity

450   (right Y axis, grey bars) of RTgill-W1 cells following exposure to effluents collected in weeks 1-

451   5. Asterisks denote statistical significance at p<0.05.

452

453   As effects were observed on the epithelial integrity, and because the gill is a site of xenobiotic

454   uptake and detoxification, the effects of the effluents on the gene expression of zonula

455   occludens-1 (ZO-1) tight junction protein and multixenobiotic resistance genes in RTgill-W1

456   cells were studied. The ZO-1 gene was selected due to the decreased epithelial integrity observed

457   in the paracellular permeability assay. Results showed ZO-1 mRNA levels were elevated after

458   exposure to effluents collected on week 1 and 3 (SI; Figure S7). Previous studies have shown

459   that the RTgill-W1 cells express functional tight junctions that can respond to certain

460   modulators[67]. In the current study, the RTgill-W1 cell model in transwell inserts showed an

461   increased paracellular permeability followed by an increase in ZO-1 expression upon exposure to

462   week 3 effluent, suggesting an impact on the epithelial integrity and a compromised barrier

463   function. Moreover, the DCFH-DA assay indicated exposure to the week 3 effluent led to a 2-

464 fold increase in ROS formation, suggesting a ROS-induced compromised epithelial integrity. It

465 has previously been shown that oxidative stress can lead to a disruption of tight junctions in

466 MDCK canine kidney cells[68].

467 The multixenobiotic resistance (MXR) mechanism mediated by ATP binding cassette

468 transporters is an important mechanism of defense against xenobiotics, which functions by

469 extruding them or their metabolites out of the cell. The transporters are localized in tissues with a

470 barrier function or involved in secretion and absorption, they transport a wide variety of

471 compounds across cell membranes and it has recently been shown that NPs, including Ag NPs,

472 can interfere with the MXR system[69,70]. Due to their importance in cellular defense against

473 xenobiotics, the multixenobiotic resistance genes ABCB1, ABCC1, ABBC2 were also

474 investigated in the current study. Exposure to the effluents led to increased mRNA levels of

475 ABCB1, ABCC1 and ABCC2 transporters, with ABCB1 (the most responsive) exhibiting

476 increased expression levels in response to effluents from weeks 1-3 (3.4-fold increase upon

477 exposure to effluent week 2) (SI; Figure S7). These results indicate an interference with the

478 defense mechanism and potentially compromised protection against xenobiotics. The

479 contribution of other trace elements and other unidentified stressors present in the effluent to the

480 observed effects cannot be excluded. It also remains to be determined whether this observed

481 change in gene expression also leads to transporter functional changes.

482 **Environmental implications**. The combination of a lab-scale WWTP with detailed fractionation

483 approaches, characterization techniques (TEM, sp-ICP-MS, sequential filtration/ICP-MS), a

484 battery of marine and freshwater bioassays and an *in vitro* gill cell line model allowed the effects

485 of transformed NPs to be investigated. This study shows that Ag NPs are transformed through

486 simulated biological WWTP processes to particles associated with S, Cu and Zn. The resulting

487   hazard cannot be predicted based on exposures made in simplified media or determined by

488   measuring the NP concentration and the dissolved fraction since the effluent is complex with

489   additional stressors (e.g suspended solids, NH_4) either exacerbating or mitigating the effects

490   depending on the organism, endpoint and media used. The transformed particles appeared to

491   have a greater impact on epibentic copepods suggesting that they were still bioavailable despite

492   their transformation. Differences in responses in marine vs freshwater algae and crustaceans

493   highlight the importance of the media composition in the NP speciation that can lead to species-

494   specific responses. The study reinforces the need to use multiple test species representing

495   different environments and exposure routes, bioassays and endpoints to gain clearer

496   understanding of the potential hazards of low level realistic concentrations of transformed

497   nanomaterials and multiple stressors in environmental media of increased complexity. The

498   results highlighting the difference in toxicity of pristine and transformed particles, emphasize the

499   need for future studies using a broader range of weathered or transformed NPs in relevant

500   exposure scenarios to provide a more accurate understanding of their potential impacts. The

501   combination of complementary analytical techniques (TEM, sp-ICP-MS, sequential

502   filtration/ICP-MS) was useful for the detection and characterization of low NPs concentrations in

503   complex environmental matrices. Our results demonstrated that Ag and TiO_2 NPs show a strong

504   association with solids, suggesting the potential for terrestrial organisms' exposure through

505   biosolid[21,42,71] application. Based on these conclusions future studies should focus on the effects

506   of transformed NPs associated with the biosolids on terrestrial organisms and the factors

507   contributing to species-specific responses.

508

509   ASSOCIATED CONTENT

510   **Supporting Information**. Additional information is provided for the synthetic wastewater

511   composition, the lab-scale WWTP description and operation (and schematic; Figure S1), sample

512   preparation description for STEM/EDS and sp-ICP-MS, mass balance calculations for Ag and

513   TiO_2 NPs, DLS measurements of TiO_2 and Ag NPs stock dispersions in MilliQ water, synthetic

514   wastewater, seawater and exposure media, sp-ICP-MS measurements of NP stock dispersions

515   and effluents (Table S1), characteristics of the effluents collected in weeks 1-5 (Table S2) and an

516   overview of genes, primer sequences and protocol used for qPCR (Table S3). In addition, TEM

517   images of Ag and TiO_2 NPs stock dispersions are provided (Figure S2, S3), fractionation of Ti

518   (Figure S4), effects of effluents on *S. pseudocostatum* and *R. subcapitata* ROS formation (Figure

519   S5), effects of effluents on RTgill-W1 ROS formation (Figure S6), gene expression (Figure S7)

520   and principal component analysis (PCA) of the physicochemical parameters and effects observed

521   in the different bioassays (Figure S8).

522

523   AUTHOR INFORMATION

524   **Corresponding Author**

525   * Anastasia Georgantzopoulou. E-mail: anastasia.georgantzopoulou@niva.no. Tel: +4798227741

526   **Author Contributions**

527   The manuscript was written through contributions of all authors. All authors have given approval

528   to the final version of the manuscript.

529

530   ACKNOWLEDGMENT

REFERENCES

(1)   Weir, A.; Westerhoff, P.; Fabricius, L.; Hristovski, K.; Von Goetz, N. Titanium Dioxide Nanoparticles in Food and Personal Care Products. *Environ. Sci. Technol.* **2012**, *46* (4), 2242–2250.

(2)   Voelker, D.; Schlich, K.; Hohndorf, L.; Koch, W.; Kuehnen, U.; Polleichtner, C.; Kussatz, C.; Hund-Rinke, K. Approach on Environmental Risk Assessment of Nanosilver Released from Textiles. *Environ. Res.* **2015**, *140*, 661–672.

(3)   Kiser, M. A.; Westerhoff, P.; Benn, T.; Wang, Y.; Pérez-Rivera, J.; Hristovski, K. Titanium Nanomaterial Removal and Release from Wastewater Treatment Plants. *Environ. Sci. Technol.* **2009**, *43* (17), 6757–6763.

(4)   Li, L.; Hartmann, G.; Döblinger, M.; Schuster, M. Quantification of Nanoscale Silver Particles Removal and Release from Municipal Wastewater Treatment Plants in Germany. *Environ. Sci. Technol.* **2013**, *47*, 7317–7323.

(5)   Johnson, A. C.; Jürgens, M. D.; Lawlor, A. J.; Cisowska, I.; Williams, R. J. Particulate and Colloidal Silver in Sewage Effluent and Sludge Discharged from British Wastewater Treatment Plants. *Chemosphere* **2014**, *112*, 49–55.

(6)   Westerhoff, P.; Song, G.; Hristovski, K.; Kiser, M. A. Occurrence and Removal of Titanium at Full Scale Wastewater Treatment Plants: Implications for TiO_2 Nanomaterials. *J. Environ. Monit.* **2011**, *13* (5), 1195.

(7)   Polesel, F.; Farkas, J.; Kjos, M.; Almeida Carvalho, P.; Flores-Alsina, X.; Gernaey, K. V;

564   Foss Hansen, S.; Plosz, B. G.; Booth, A. M. Occurrence, Characterisation and Fate of

565   (Nano)Particulate Ti and Ag in Two Norwegian Wastewater Treatment Plants. *Water Res.*

566   **2018**, *141*, 19–31.

567   (8) Kaegi, R.; Voegelin, A.; Ort, C.; Sinnet, B.; Thalmann, B.; Krismer, J.; Hagendorfer, H.;

568   Elumelu, M.; Mueller, E. Fate and Transformation of Silver Nanoparticles in Urban

569   Wastewater Systems. *Water Res.* **2013**, *47* (12), 3866–3877.

570   (9) Li, L.; Stoiber, M.; Wimmer, A.; Xu, Z.; Lindenblatt, C.; Helmreich, B.; Schuster, M. To

571   What Extent Can Full-Scale Wastewater Treatment Plant Effluent Influence the

572   Occurrence of Silver-Based Nanoparticles in Surface Waters? *Environ. Sci. Technol.*

573   **2016**, *50* (12), 6327–6333.

574   (10) Azodi, M.; Sultan, Y.; Ghoshal, S. Dissolution Behavior of Silver Nanoparticles and

575   Formation of Secondary Silver Nanoparticles in Municipal Wastewater by Single-Particle

576   ICP-MS. *Environ. Sci. Technol.* **2016**, *50* (24), 13318–13327.

577   (11) Levard, C.; Hotze, E. M.; Lowry, G. V; Brown, G. E. Environmental Transformations of

578   Silver Nanoparticles: Impact on Stability and Toxicity. *Environ. Sci. Technol.* **2012**, *46*

579   (13), 6900–6914.

580   (12) Azimzada, A.; Tufenkji, N.; Wilkinson, K. J. Transformations of Silver Nanoparticles in

581   Wastewater Effluents: Links to Ag Bioavailability. *Environ. Sci. Nano* **2017**, *4*, 1339–

582   1349.

583   (13) Kent, R. D.; Oser, J. G.; Vikesland, P. J. Controlled Evaluation of Silver Nanoparticle

584   Sulfidation in a Full-Scale Wastewater Treatment Plant. *Environ. Sci. Technol.* **2014**, *48*

585   (15), 8564–8572.

586   (14)   Kaegi, R.; Voegelin, A.; Sinnet, B.; Zuleeg, S.; Hagendorfer, H.; Burkhardt, M.; Siegrist,

587   H. Behavior of Metallic Silver Nanoparticles in a Pilot Wastewater Treatment Plant.

588   *Environ. Sci. Technol.* **2011**, *45* (9), 3902–3908.

589   (15)   Lin, S.; Taylor, A. a.; Ji, Z.; Chang, C. H.; Kinsinger, N. M.; Ueng, W.; Walker, S. L.;

590   Nel, A. E. Understanding the Transformation, Speciation, and Hazard Potential of Copper

591   Particles in a Model Septic Tank System Using Zebrafish to Monitor the Effluent. *ACS*

592   *Nano* **2015**, *9* (2), 2038–2048.

593   (16)   Holden, P. A.; Gardea-Torresdey, J. L.; Klaessig, F.; Turco, R. F.; Mortimer, M.; Hund-

594   Rinke, K.; Cohen Hubal, E. A.; Avery, D.; Barceló, D.; Behra, R.; Cohen, Y.; Deydier-

595   Stephan, L.; Ferguson, P. L.; Fernandes, T. F.; Herr Harthorn, B.; Henderson, W. M.;

596   Hoke, R. A.; Hristozov, D.; Johnston, J. M.; et al. Considerations of Environmentally

597   Relevant Test Conditions for Improved Evaluation of Ecological Hazards of Engineered

598   Nanomaterials. *Environ. Sci. Technol.* **2016**, *50* (12), 6124–6145.

599   (17)   Kühr, S.; Schneider, S.; Meisterjahn, B.; Schlich, K.; Hund-Rinke, K.; Schlechtriem, C.

600   Silver Nanoparticles in Sewage Treatment Plant Effluents: Chronic Effects and

601   Accumulation of Silver in the Freshwater Amphipod *Hyalella Azteca*. *Environ. Sci. Eur.*

602   **2018**, *30* (1), 1–11.

603   (18)   Bruneau, A.; Turcotte, P.; Pilote, M.; Gagné, F.; Gagnon, C. Fate of Silver Nanoparticles

604   in Wastewater and Immunotoxic Effects on Rainbow Trout. *Aquat. Toxicol.* **2016**, *174*,

605   70–81.

606   (19)   Thalmann, B.; Voegelin, A.; Von Gunten, U.; Behra, R.; Morgenroth, E.; Kaegi, R. Effect

607   of Ozone Treatment on Nano-Sized Silver Sulfide in Wastewater Effluent. *Environ. Sci.*

608   *Technol.* **2015**, *49* (18), 10911–10919.

609   (20)   Muth-Köhne, E.; Sonnack, L.; Schlich, K.; Hischen, F.; Baumgartner, W.; Hund-Rinke,

610   K.; Schäfers, C.; Fenske, M. The Toxicity of Silver Nanoparticles to Zebrafish Embryos

611   Increases through Sewage Treatment Processes. *Ecotoxicology* **2013**, *22* (8), 1264–1277.

612   (21)   Kampe, S.; Kaegi, R.; Schlich, K.; Wasmuth, C.; Hollert, H.; Schlechtriem, C. Silver

613   Nanoparticles in Sewage Sludge: Bioavailability of Sulfidized Silver to the Terrestrial

614   Isopod *Porcellio Scaber*. *Environ. Toxicol. Chem.* **2018**, *9999* (9999), 1–8.

615   (22)   Kraas, M.; Schlich, K.; Knopf, B.; Wege, F.; Kägi, R.; Terytze, K.; Hund-Rinke, K. Long-

616   Term Effects of Sulfidized Silver Nanoparticles in Sewage Sludge on Soil Microflora.

617   *Environ. Toxicol. Chem.* **2017**, *36* (12), 3305–3313.

618   (23)   Pradas del Real, A. E.; Vidal, V.; Carrière, M.; Castillo-Michel, H.; Levard, C.; Chaurand,

619   P.; Sarret, G. Silver Nanoparticles and Wheat Roots: A Complex Interplay. *Environ. Sci.*

620   *Technol.* **2017**, *51* (10), 5774–5782.

621   (24)   Laux, P.; Riebeling, C.; Booth, A. M.; Brain, J. D.; Brunner, J.; Cerrillo, C.; Creutzenberg,

622   O.; Estrela-Lopis, I.; Gebel, T.; Johanson, G.; Jungnickel, H.; Kock, H.; Tentschert, J.;

623   Tlili, A.; Schäffer, A.; Sips, A. J. A. M.; Yokel, R. A.; Luch, A. Challenges in

624   Characterizing the Environmental Fate and Effects of Carbon Nanotubes and Inorganic

625   Nanomaterials in Aquatic Systems. *Environ. Sci. Nano* **2017**, *5*, 48–63.

626   (25)   Weltje, L.; Sumpter, J. P. What Makes a Concentration Environmentally Relevant?

627   Critique and a Proposal. *Environ. Sci. Technol.* **2017**, *51* (20), 11520–11521.

628   (26)   Baker, T. J.; Tyler, C. R.; Galloway, T. S. Impacts of Metal and Metal Oxide

629   Nanoparticles on Marine Organisms. *Environ. Pollut.* **2014**, *186*, 257–271.

630   (27)   Joint Research Centre of the European Commission. *Titanium Dioxide, NM-100, NM-101,*

631   *NM-102, NM-103, NM-104, NM-105: Characterisation and Physico- Chemical*

632   *Properties*; 2014.

633   (28)   Jensen, K.; Booth, A.; Kembouche, Y.; Boraschi, D. NANoREG Deliverable 2.06.

634   Validated Protocols for Test Item Preparation for Key in Vitro and Ecotoxicity Studies.

635   *NANoREG*. 2016, p 77.

636   (29)   Peters, R.; Herrera-Rivera, Z.; Undas, A.; Van Der Lee, M.; Marvin, H.; Bouwmeester,

637   H.; Weigel, S. Single Particle ICP-MS Combined with a Data Evaluation Tool as a

638   Routine Technique for the Analysis of Nanoparticles in Complex Matrices. *J. Anal. At.*

639   *Spectrom.* **2015**, *30*, 1274–1285.

640   (30)   International Organisation for Standardization (ISO). Water Quality- Marine Algal

641   Growth Inhibition Test with *Skeletonema Costatum* and *Phaeodactylum Tricornutum* (ISO

642   10253). 2006.

643   (31)   Miller, R. J.; Lenihan, H. S.; Muller, E. B.; Tseng, N.; Hanna, S. K.; Keller, A. A. Impacts

644   of Metal Oxide Nanoparticles on Marine Phytoplankton. *Environ. Sci. Technol.* **2010**, *44*

645   (19), 7329–7334.

646   (32)   Organisation for Economic Co-operation and Development (OECD). OECD Guidelines

647   for the Testing of Chemicals/Test 201: Alga, Growth Inhibition Test. **1984**, No. June.

648   (33)   Organisation for Economic Co-operation and Development (OECD). OECD Guidelines

649   for the Testing of Chemicals/ Section 2: Effects on Biotic Systems, Test No. 202: *Daphnia*

650   Sp. Acute Immobilisation Test. **2004**.

651   (34)   Georgantzopoulou, A.; Balachandran, Y. L.; Rosenkranz, P.; Dusinska, M.; Lankoff, A.;

652   Wojewodzka, M.; Kruszewski, M.; Guignard, C.; Audinot, J.-N.; Girija, S.; Hoffmann, L.;

653   Gutleb, A. C. Ag Nanoparticles: Size- and Surface-Dependent Effects on Model Aquatic

654   Organisms and Uptake Evaluation with NanoSIMS. *Nanotoxicology* **2013**, *7* (7), 1168–

655   1178.

656   (35)   United States Environmental Protection Agency. Methods for Measuring the Acute

657   Toxicity of Effluents and Receiving Waters to Freshwater and Marine Organisms. **2002**,

658   No. October, 266.

659   (36)   Macken, A.; Lillicrap, A.; Langford, K. Benzoylurea Pesticides Used as Veterinary

660   Medicines in Aquaculture: Risks and Developmental Effects on Nontarget Crustaceans.

661   *Environ. Toxicol. Chem.* **2015**, *34* (7), 1533–1542.

662   (37)   Schirmer, K.; Chan, A. G. J.; Greenberg, B. M.; Dixon, D. G.; Bols, N. C. Methodology

663   for Demonstrating and Measuring the Photocytotoxicity of Fluoranthene to Fish Cells in

664   Culture. *Toxicol. Vitr.* **1997**, *11* (1–2), 107–119.

665   (38)   Yue, Y.; Behra, R.; Sigg, L.; Fernández Freire, P.; Pillai, S.; Schirmer, K. Toxicity of

666   Silver Nanoparticles to a Fish Gill Cell Line: Role of Medium Composition.

667   *Nanotoxicology* **2015**, *9* (1), 54–63.

668   (39)   Hultman, M. T.; Song, Y.; Tollefsen, K. E. 17α-Ethinylestradiol (EE2) Effect on Global

669   Gene Expression in Primary Rainbow Trout (*Oncorhynchus Mykiss*) Hepatocytes. *Aquat.*

670   *Toxicol.* **2015**, *169*, 90–104.

671   (40)   Domingos, R. F.; Baalousha, M. A.; Ju-Nam, Y.; Reid, M. M.; Tufenkji, N.; Lead, J. R.;

672   Leppard, G. G.; Wilkinson, K. J. Characterizing Manufactured Nanoparticles in the

673   Environment: Multimethod Determination of Particle Sizes. *Environ. Sci. Technol.* **2009**,

674   *43*, 7277–7284.

675   (41)   Wang, Y.; Westerhoff, P.; Hristovski, K. D. Fate and Biological Effects of Silver,

676   Titanium Dioxide, and C 60 (Fullerene) Nanomaterials during Simulated Wastewater

677   Treatment Processes. *J. Hazard. Mater.* **2012**, *201–202*, 16–22.

678   (42)   Kim, B.; Park, C. S.; Murayama, M.; Hochella, M. F. Discovery and Characterization of

679   Silver Sulfide Nanoparticles in Final Sewage Sludge Products. *Environ. Sci. Technol.*

680   **2010**, *44* (19), 7509–7514.

681   (43)   Gondikas, A. P.; Von Der Kammer, F.; Reed, R. B.; Wagner, S.; Ranville, J. F.; Hofmann,

682   T. Release of TiO2 Nanoparticles from Sunscreens into Surface Waters: A One-Year

683   Survey at the Old Danube Recreational Lake. *Environ. Sci. Technol.* **2014**, *48* (10), 5415–

684   5422.

685   (44)   Tuoriniemi, J.; Cornelis, G.; Hassellöv, M. Size Discrimination and Detection Capabilities

686   of Single-Particle ICPMS for Environmental Analysis of Silver Nanoparticles. *Anal.*

687   *Chem.* **2012**, *84* (9), 3965–3972.

688   (45)   Mitrano, D. M.; Lesher, E. K.; Bednar, A.; Monserud, J.; Higgins, C. P.; Ranville, J. F.

689   Detecting Nanoparticulate Silver Using Single-Particle Inductively Coupled Plasma-Mass

690   Spectrometry. *Environ. Toxicol. Chem.* **2012**, *31* (1), 115–121.

691   (46)   Hadioui, M.; Merdzan, V.; Wilkinson, K. J. Detection and Characterization of ZnO

692   Nanoparticles in Surface and Waste Waters Using Single Particle ICPMS. *Environ. Sci.*

693   *Technol.* **2015**, *49* (10), 6141–6148.

694   (47)   Lee, S.; Bi, X.; Reed, R. B.; Ranville, J. F.; Herckes, P.; Westerhoff, P. Nanoparticle Size

695   Detection Limits by Single Particle ICP-MS for 40 Elements. *Environ. Sci. Technol.* **2014**,

696   *48* (17), 10291–10300.

697   (48)   Mallevre, F.; Alba, C.; Milne, C.; Gillespie, S.; Fernandes, T.; Aspray, T. Toxicity Testing

698   of Pristine and Aged Silver Nanoparticles in Real Wastewaters Using Bioluminescent

699   *Pseudomonas Putida*. *Nanomaterials* **2016**, *6* (3), 49.

700   (49)   Saison, C.; Perreault, F.; Daigle, J. C.; Fortin, C.; Claverie, J.; Morin, M.; Popovic, R.

701   Effect of Core-Shell Copper Oxide Nanoparticles on Cell Culture Morphology and

702   Photosynthesis (Photosystem II Energy Distribution) in the Green Alga, *Chlamydomonas*

703   *Reinhardtii*. *Aquat. Toxicol.* **2010**, *96* (2), 109–114.

704   (50)   Oukarroum, A.; Bras, S.; Perreault, F.; Popovic, R. Inhibitory Effects of Silver

705   Nanoparticles in Two Green Algae, *Chlorella Vulgaris* and *Dunaliella Tertiolecta*.

706   *Ecotoxicol. Environ. Saf.* **2012**, *78*, 80–85.

707   (51)   Zaytseva, O.; Neumann, G. Carbon Nanomaterials: Production, Impact on Plant

708   Development, Agricultural and Environmental Applications. *Chem. Biol. Technol. Agric.*

709   **2016**, *3* (1), 17.

710 (52) Taylor, C.; Matzke, M.; Kroll, A.; Read, D. S.; Svendsen, C.; Crossley, A. Toxic

711 Interactions of Different Silver Forms with Freshwater Green Algae and Cyanobacteria

712 and Their Effects on Mechanistic Endpoints and the Production of Extracellular Polymeric

713 Substances. *Environ. Sci. Nano* **2016**, *3* (2), 396–408.

714 (53) Levard, C.; Hotze, E. M.; Colman, B. P.; Dale, A. L.; Truong, L.; Yang, X. Y.; Bone, A.

715 J.; Brown, G. E.; Tanguay, R. L.; Di Giulio, R. T.; Bernhardt, E. S.; Meyer, J. N.;

716 Wiesner, M. R.; Lowry, G. V. Sulfidation of Silver Nanoparticles: Natural Antidote to

717 Their Toxicity. *Environ. Sci. Technol.* **2013**, *47* (23), 13440–13448.

718 (54) Gophen, M.; Geller, W. Filter Mesh Size and Food Particle Uptake by *Daphnia*.

719 *Oecologia* **1984**, *64* (3), 408–412.

720 (55) Williams, T. Survival and Development of Copepod Larvae *Tisbe Battagliai* in Surface

721 Microlayer, Water and Sediment Elutriates from the German Bight. *Mar. Ecol. Prog. Ser.*

722 **1992**, *91*, 221–228.

723 (56) Puello☐Cruz, A. C.; Mezo☐Villalobos, S.; Voltolini, D. Progeny Production of the

724 Copepods *Pseudodiaptomus Euryhalinus* and *Tisbe Monozota* in Monospecific and Mixed

725 Cultures. *J. world Aquac. Soc.* **2013**, *44* (3), 447–454.

726 (57) Liu, J.; Hurt, R. H. Ion Release Kinetics and Particle Persistence in Aqueous Nano-Silver

727 Colloids. *Environ. Sci. Technol.* **2010**, *44* (6), 2169–2175.

728 (58) Loza, K.; Diendorf, J.; Sengstock, C.; Ruiz-Gonzalez, L.; Gonzalez-Calbet, J. M.; Vallet-

729 Regi, M.; Köller, M.; Epple, M. The Dissolution and Biological Effects of Silver

730 Nanoparticles in Biological Media. *J. Mater. Chem. B* **2014**, *2* (12), 1634.

731 (59) Navarro, E.; Piccapietra, F.; Wagner, B.; Marconi, F.; Kaegi, R.; Odzak, N.; Sigg, L.;

732   Behra, R. Toxicity of Silver Nanoparticles to *Chlamydomonas Reinhardtii*. *Environ. Sci.*

733   *Technol.* **2008**, *42* (23), 8959–8964.

734 (60) Zhao, C.-M.; Wang, W.-X. Comparison of Acute and Chronic Toxicity of Silver

735   Nanoparticles and Silver Nitrate to *Daphnia Magna*. *Environ. Toxicol. Chem.* **2011**, *30*

736   (4), 885–892.

737 (61) Köser, J.; Engelke, M.; Hoppe, M.; Nogowski, A.; Filser, J.; Thöming, J. Predictability of

738   Silver Nanoparticle Speciation and Toxicity in Ecotoxicological Media. *Environ. Sci.*

739   *Nano* **2017**, *4* (7), 1470–1483.

740 (62) Bury, N. R.; Schnell, S.; Hogstrand, C. Gill Cell Culture Systems as Models for Aquatic

741   Environmental Monitoring. *J. Exp. Biol.* **2014**, *217*, 639–650.

742 (63) Lee, L. E. J.; Dayeh, V. R.; Schirmer, K.; Bols, N. C. Applications and Potential Uses of

743   Fish Gill Cell Lines: Examples with RTgill-W1. *Vitr. Cell. Dev. Biol. - Anim.* **2009**, *45* (3–

744   4), 127–134.

745 (64) Minghetti, M.; Schnell, S.; Chadwick, M. A.; Hogstrand, C.; Bury, N. R. A Primary FIsh

746   Gill Cell System (FIGCS) for Environmental Monitoring of River Waters. *Aquat. Toxicol.*

747   **2014**, *154*, 184–192.

748 (65) Walker, P. A.; Kille, P.; Hurley, A.; Bury, N. R.; Hogstrand, C. An *in Vitro* Method to

749   Assess Toxicity of Waterborne Metals to Fish. *Toxicol. Appl. Pharmacol.* **2008**, *230* (1),

750   67–77.

751   (66)   Farkas, J.; Christian, P.; Gallego-Urrea, J. A.; Roos, N.; Hasellöv, M.; Tollefsen, K. E.;

752   Thomas, K. V. Uptake and Effects of Manufactured Silver Nanoparticles in Rainbow

753   Trout (*Oncorhynchus Mykiss*) Gill Cells. *Aquat. Toxicol.* **2011**, *101* (1), 117–125.

754   (67)   Trubitt, R. T.; Rabeneck, D. B.; Bujak, J. K.; Bossus, M. C.; Madsen, S. S.; Tipsmark, C.

755   K. Transepithelial Resistance and Claudin Expression in Trout RTgill-W1 Cell Line:

756   Effects of Osmoregulatory Hormones. *Comp. Biochem. Physiol. -Part A Mol. Integr.*

757   *Physiol.* **2015**, *182*, 45–52.

758   (68)   Meyer, T. N.; Schwesinger, C.; Ye, J.; Denker, B. M.; Nigam, S. K. Reassembly of the

759   Tight Junction after Oxidative Stress Depends on Tyrosine Kinase Activity. *J. Biol. Chem.*

760   **2001**, *276* (25), 22048–22055.

761   (69)   Georgantzopoulou, A.; Cambier, S.; Serchi, T.; Kruszewski, M.; Balachandran, Y. L.;

762   Grysan, P.; Audinot, J. N.; Ziebel, J.; Guignard, C.; Gutleb, A. C.; Murk, A. T. J.

763   Inhibition of Multixenobiotic Resistance Transporters (MXR) by Silver Nanoparticles and

764   Ions *in Vitro* and in *Daphnia Magna*. *Sci. Total Environ.* **2016**, *569–570* (0349), 681–689.

765   (70)   Wu, B.; Torres-Duarte, C.; Cole, B. J.; Cherr, G. N. Copper Oxide and Zinc Oxide

766   Nanomaterials Act as Inhibitors of Multidrug Resistance Transport in Sea Urchin

767   Embryos: Their Role as Chemosensitizers. *Environ. Sci. Technol.* **2015**, *49*, 5760–5770.

768   (71)   Yang, Y.; Wang, Y.; Westerhoff, P.; Hristovski, K.; Jin, V. L.; Johnson, M. V. V; Arnold,

769   J. G. Metal and Nanoparticle Occurrence in Biosolid-Amended Soils. *Sci. Total Environ.*

770   **2014**, *485–486* (1), 441–449.

771
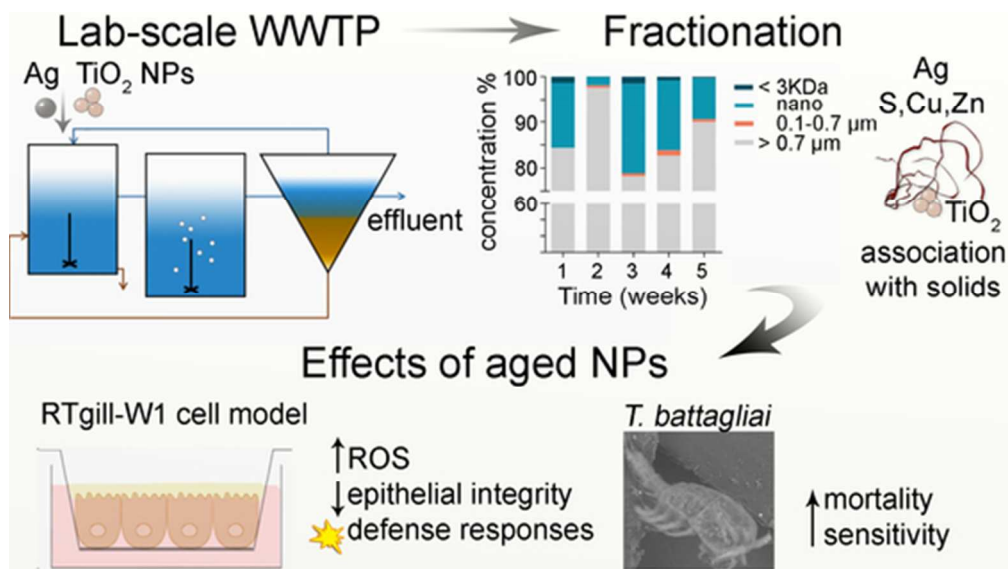
Graphical abstract

47x26mm (300 x 300 DPI)